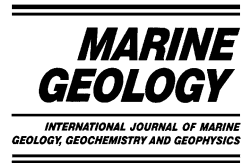




ELSEVIER

Marine Geology 184 (2002) 143–162



www.elsevier.com/locate/margeo

# Seismic stratigraphy of the Frontal Hawaiian Moat: implications for sedimentary processes at the leading edge of an oceanic hotspot trace

Stephen C. Leslie<sup>a,\*</sup>, Gregory F. Moore<sup>a</sup>, Julia K. Morgan<sup>b</sup>,  
Denise J. Hills<sup>a</sup>

<sup>a</sup> Department of Geology and Geophysics, University of Hawaii, Honolulu, HI 96822, USA

<sup>b</sup> Department of Geology and Geophysics, Rice University, Houston, TX 77005, USA

Received 13 February 2001; accepted 15 October 2001

## Abstract

Multi-channel seismic imaging reveals the seismic stratigraphy and associated sedimentary processes of the Frontal Hawaiian Moat (FHM) to the southeast of the island of Hawaii. Two sedimentary units are defined: (1) a basal layer of pelagic sediment draping the oceanic basement and (2) a wedge of volcanoclastic material infilling the FHM and onlapping the Frontal Hawaiian Arch. Three distinct seismic facies within the volcanoclastic unit are recognized: (A) areas of chaotic or incoherent reflections interpreted as proximal debris avalanche or slump deposits; (B) groups of hummocky and distorted reflections interpreted as distal debris avalanche or debris flow deposits; and (C) regions of parallel and laterally continuous reflections interpreted as turbidite deposits. The distribution of these facies delineates slope apron, proximal basin, and distal basin depositional environments (respectively) within the FHM. The northwest drift of the Pacific Plate over the Hawaiian hot spot results in the apparent southeasterly migration of the Hawaiian chain. Advancement of the depositional environments within the FHM occurs as individual volcanoes evolve, erode, and are superseded by new volcanic centers. The interplay between depositional processes and tectonic forces (plate motion and lithospheric flexure) predicts a coarsening-upward stratigraphy within the FHM. The combined accumulation of pelagic and volcanoclastic sediment defines a heterogeneous, and potentially unstable, layer of low strength material beneath the volcanic edifice that may influence the mobility of the island flanks. © 2002 Elsevier Science B.V. All rights reserved.

*Keywords:* Hawaii; landslides; volcanoclastic sediment; turbidite; seismic stratigraphy; Ocean Drilling Program

## 1. Introduction

Giant submarine landslides have been well

documented on the flanks of volcanic islands such as the Hawaiian Islands, the Canaries, and La Réunion (e.g. Moore et al., 1989; Watts and Masson, 1995; Funck and Lykke-Anderson, 1998; de Voogd et al., 1999). Deep-sea volcanoclastic sediment that surrounds oceanic volcanoes is derived from these giant landslides as well as smaller mass-wasting events (e.g. Menard, 1956;

\* Corresponding author. Tel.: +1-808-956-6082;  
Fax: +1-808-956-5154.

E-mail address: sleslie@soest.hawaii.edu (S.C. Leslie).

Rees et al., 1993; Wolfe et al., 1994; Lucci and Kidd, 1998; Funck and Schmincke, 1998; Masson et al., 1998; Ollier et al., 1998; Urgeles et al., 1998). In Hawaii, landslides may occur throughout the life of an individual volcano, but the largest events appear to occur at or near the end of the shield-building stage (Moore et al., 1989). Sediments from such prodigious landslides can range from large-scale debris avalanche deposits up to 2 km thick and 230 km long (Moore et al., 1994) to centimeter-thick turbidite deposits located >900 km to the south of the Hawaiian Islands (Rehm and Halbach, 1982; Garcia and Hull, 1994).

Flexural moats often form around oceanic volcanoes in response to lithospheric loading (Menard, 1964). The Frontal Hawaiian Moat (FHM), southeast of the island of Hawaii, is the youngest expression of the Hawaiian Moat (Fig. 1). Widespread mass wasting from the leading (southeast) edge of the Hawaiian Ridge contributes sediments to the FHM (Moore and Clague, 1992; Smith et al., 1999; Naka et al., 2002). These sediments will eventually be covered by later volcanoes of the Hawaiian Ridge, as the Pacific plate drifts to the northwest over the Hawaiian hot-spot (Morgan, 1971; Dalrymple et al., 1973). Thus, sediments infilling the FHM not only record the landslide history of the nearby volcanic slopes, but are modern analogs to deposits that have been buried beneath the volcanoes of the Hawaiian Islands.

Sedimentary layers underlying ocean island volcanoes are thought to facilitate the formation of detachment surfaces or décollements that enable the mobilization of large portions of the volcanic flanks of oceanic volcanoes (Denlinger and Okubo, 1995) by a process known as ‘volcanic spreading’ (Borgia, 1994). In Hawaii, the presence of a weak layer of oceanic sediment beneath the volcanoes has been invoked to explain the elongate geometry of Hawaiian rift zones (Nakamura, 1980). Analysis of reflected earthquake waves beneath the subaerial volcanic edifice reveals an 800-m-thick low-velocity layer inferred to be composed of marine sediment (Thurber and Li, 1989). In addition, recent seismic interpretations (Morgan et al., 2000) and submersible surveys

(Lipman et al., 2000) over the deep flanks of Kilauea have confirmed significant uplift and deformation at the toe of the volcanic edifice, supporting models for flank mobility that rely on a weak substrate. Voluminous submarine lava flows in the deepest part of the Hawaiian Moat near the submarine termination of the East Rift Zone (ERZ) of Kilauea and around the base of Loihi are probably interbedded within the sediment layer underlying the island edifice (Holcomb et al., 1988). Constraining the thickness and distribution of these various sedimentary and volcanic deposits is necessary to understand the growth, degradation, and deformation of oceanic volcanic islands as well as the role of landslides in the earliest stages of island building. In this study, we use multi-channel seismic (MCS) data collected on the *R/V Maurice Ewing* in 1998 (Fig. 1) to define the stratigraphy of the FHM and constrain the composition and formation of the sediment layer that underlies the island of Hawaii.

## 2. Geologic setting and previous work

The volcanic edifice of Hawaii is located at the southeast end of the Hawaiian Ridge, includes the active volcanoes Mauna Loa, Kilauea, and Loihi (a submarine volcano located 30 km southeast of Hawaii), and represents the leading edge of the Hawaiian hot spot trace (Clague and Dalrymple, 1987) (Fig. 1). The Hawaiian Islands are built upon Cretaceous age seafloor (Waggoner, 1993) that is overlain by a thin (<200 m) layer of weakly reflective pelagic sediment (Ewing et al., 1968; Winterer, 1989). The seafloor exhibits a typical north-northwest trending abyssal hill fabric that was generated during seafloor spreading (Moore and Chadwick, 1995; Macdonald et al., 1996). Lithospheric flexure induced by the weight of the volcanoes has formed a trough-like feature known as the Hawaiian Moat that surrounds the island chain. The moat is bounded by a seafloor rise known as the Hawaiian Arch, located ~250 km seaward of the island chain (Hamilton, 1957; Menard, 1964). The moat and arch have flanking segments (e.g. North Hawaiian Arch, Southern Hawaiian Moat) and frontal regions

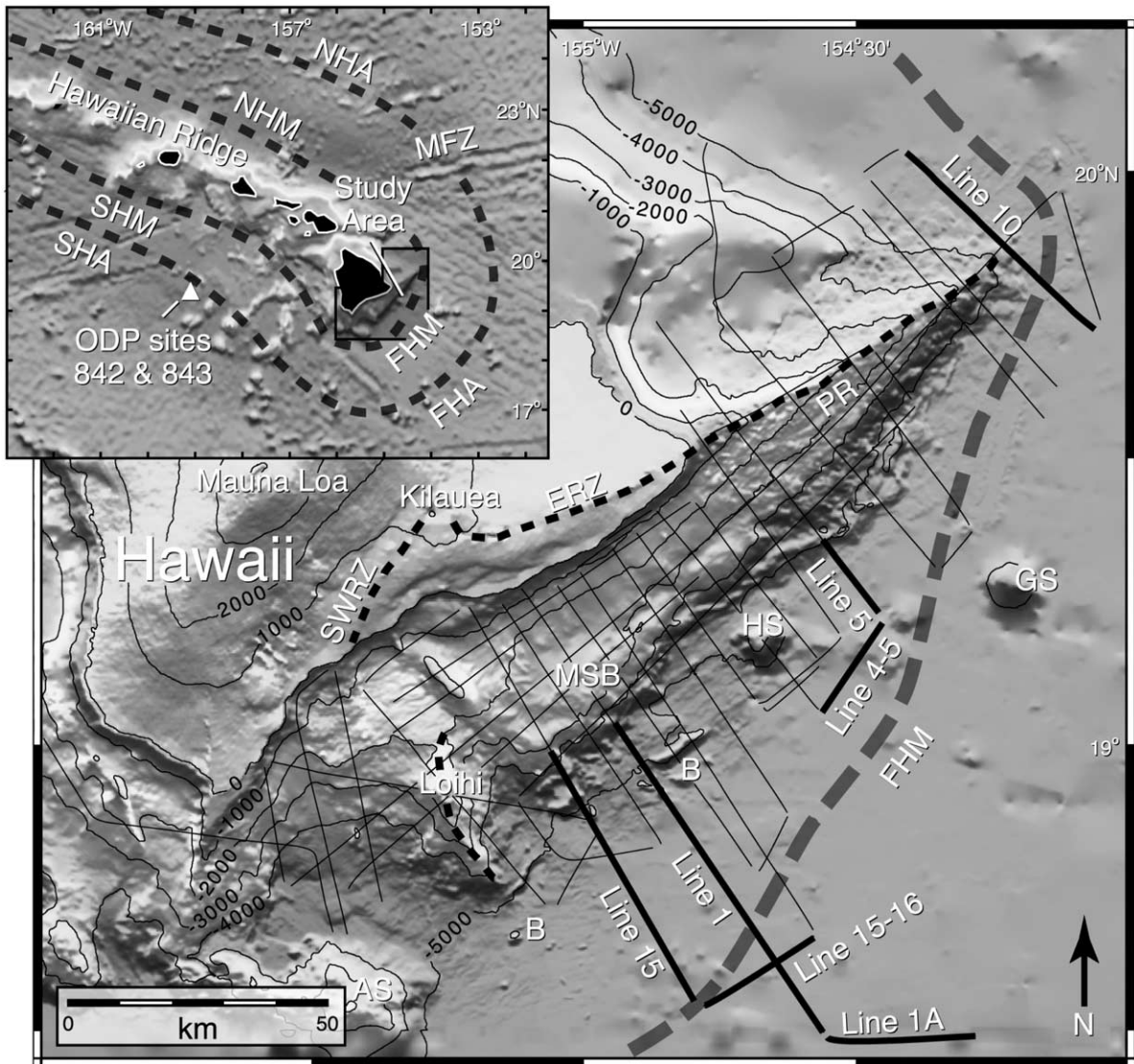


Fig. 1. Inset shows shaded relief bathymetric map of the Hawaiian Ridge and surrounding flexural moat and arch. The moat and arch are subdivided into frontal regions, i.e. the FHM and FHA, and flanking segments, i.e. the Northern and Southern Hawaiian Moat, and the Northern and Southern Hawaiian Arch. MFZ denotes Molokai fracture zone. The location of ODP Drill Sites 842 and 843 on the South Arch is indicated by triangle. Large map shows shaded relief bathymetry of the submarine slopes of the island of Hawaii. Contours in meters. Important features include the axis of FHM (thick dashed line), the ERZ of Kilauea, the Southwest Rift Zone (SWRZ) of Kilauea, the rift zones of Loihi (thinner dashed lines), the mid-slope bench of the South Flank of Kilauea (MSB), and the Puna Ridge (PR). Pre-existing seafloor topography includes Hohonu, Green and Apuupuu Seamounts (HS, GS, and AS). Isolated landslide blocks are scattered to the southeast of the volcanic edifice (B). Thin lines indicate seismic reflection profiles of entire survey. Heavy lines indicate profiles presented in this paper.

(i.e. FHM and Frontal Hawaiian Arch) (Fig. 1). In contrast to flanking segments, the FHM and Frontal Hawaiian Arch are short-lived features that will eventually be covered by the growing

Hawaiian ridge as the Pacific plate migrates across the Hawaiian hotspot locus.

Mass wasting is responsible for large-scale degradation of oceanic volcanoes and is well docu-

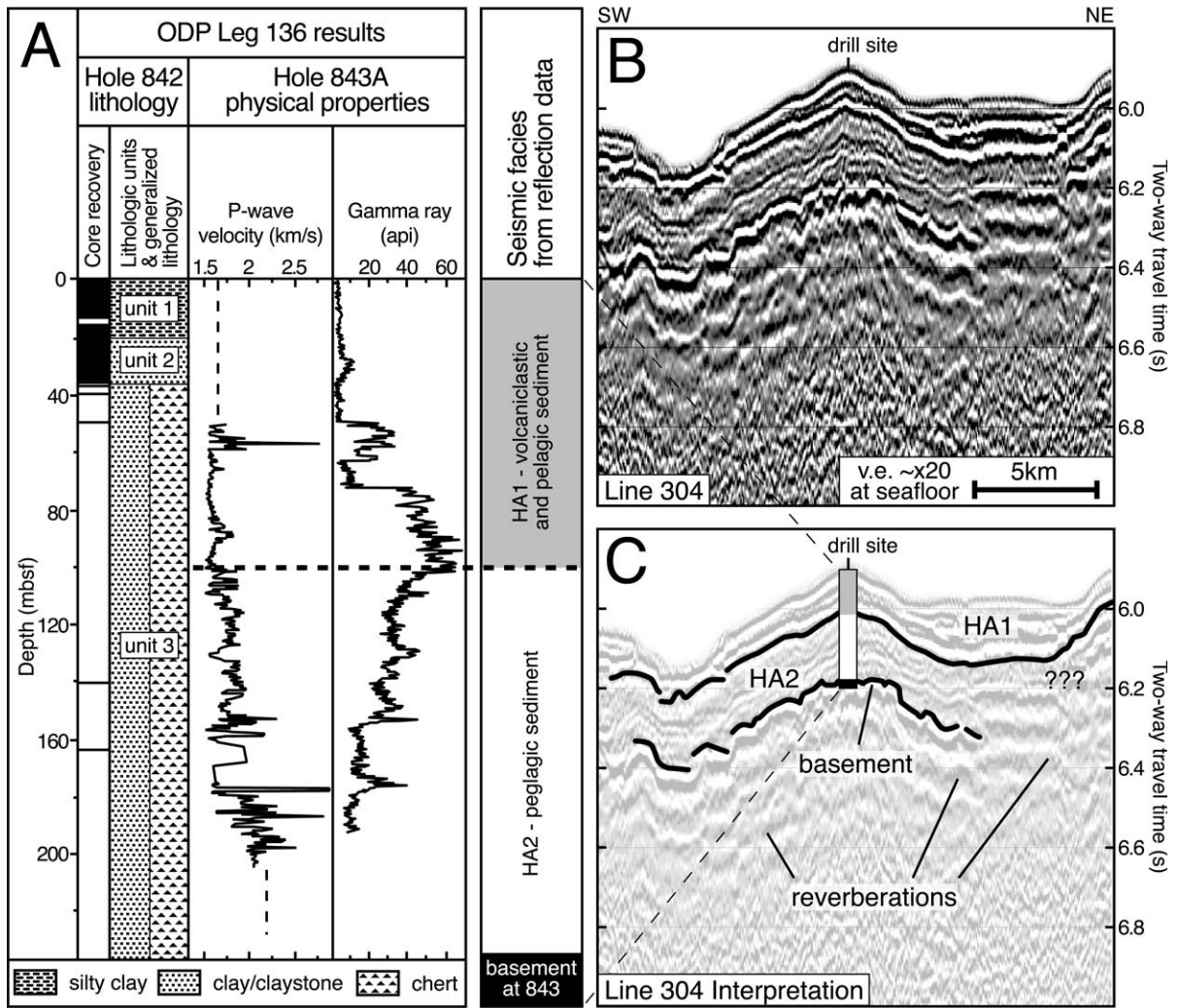


Fig. 2. Drilling results and previous seismic reflection surveys from the Southern Hawaiian Arch. (A) Lithostratigraphy and core recovery of Hole 842 matched with the physical properties of Hole 843A. The igneous basement was encountered at 228.8 mbsf at Hole 843A. Due to poor recovery of unit 3, the exact location of the boundary between volcanioclastic and pelagic sediments is unknown, but is inferred as the base of seismic layer HA1. For depth conversion purposes, velocities are inferred in the upper 50 m and lower 30 m of Hole 843A (dashed lines). (B) Seismic reflection profile RC2308-304 collected on the SHA. (C) Interpretation of reflection profile. HA1 a layer of high-amplitude, strongly continuous reflections is interpreted as distal turbidite deposits. HA2 a transparent/weakly reflective layer is interpreted as primarily pelagic sediments. Beneath HA2, a high-amplitude reflection underlain by low-frequency multiples is interpreted as the reflection from the top of the oceanic basement. Inset core is expanded and converted from time to depth domain for comparison with ODP drilling results. Note the correlation between the HA1/HA2 contact and a change in the character of the P-wave and  $\gamma$  ray logs (heavy dashed line).

mented along the Hawaiian Ridge (Moore et al., 1989). The general term ‘landslide’ or ‘landslide unit’ has been used to describe various mass movement formations ranging in size over several

orders of magnitude (Moore et al., 1989; Rees et al., 1993). Large-scale landslides (> 20 km long) identified by GLORIA sonar images have been grouped into two major types: slumps and debris

avalanches. Slumps are deeply rooted, generally coherent, bodies of rock that move incrementally or ‘creep’ downslope over an extended period (Varnes, 1978). In contrast, debris avalanches are rapidly occurring events that result in more surficial deposits that may extend for hundreds of kilometers from their source region (Moore et al., 1994). On the island of Hawaii, debris avalanche headwalls have been interpreted along the submarine slopes of Kohala, Mauna Loa, Kilauea (outer scarp of the Hilina Slump), and Loihi volcanoes (Fornari et al., 1988; Moore et al., 1989; Moore and Chadwick, 1995; Smith et al., 1999). Landslides that emplaced isolated blocks to the southeast of the island (Fig. 1) (Moore and Chadwick, 1995) likely generated smaller scale debris flow and turbidity current deposits that obscure the sea floor fabric in this region. Also present in the Hawaiian Moat are voluminous submarine lava flows surrounding the distal end of the ERZ and the base of Loihi (Holcomb et al., 1988). Because of the quantity of debris avalanche material surrounding Loihi, older lava flows around its base may have been partially or completely covered by later landslides.

Seismic reflection surveys around the Hawaiian Ridge have characterized the seismic stratigraphy of the flanking segments of the HA and Moat (Watts et al., 1985; ten Brink and Watts, 1985; Lindwall, 1988; Rees et al., 1993). These surveys imaged thick sequences of sediment partially filling the Hawaiian Moat, interpreted as primarily landslide debris. Reflections from the top of the oceanic basement vary in character from a weak reflector with rough topography underlain by low-frequency multiples (Watts et al., 1985) to a strong and discontinuous reflector (Lindwall, 1988). An extensive survey by Rees et al. (1993) defined four lithostratigraphic units infilling the Northern Hawaiian Moat: (1) a basal unit of pelagic sediments; (2) a thick wedge of lens-shaped units overlapping the Hawaiian Arch; (3) a sequence of highly reflective, continuous horizons that offlap the Hawaiian Arch; and (4) a ponded unit of near horizontal reflections confined to the deepest part of the Moat. Unit 1 was interpreted as predating the formation of the flexural moat, while units 2–4 were interpreted as the products

of mass wasting from the Hawaiian Ridge. The distribution of these deposits was explained as a function of the competing effects of sediment influx into the Moat and distributed subsidence due to loading of the lithosphere by successive volcanoes (Rees et al., 1993).

Cores obtained by the Ocean Drilling Program (ODP) Leg 136 from the Southern Hawaiian Arch furnish important groundtruth about pelagic and landslide-derived sediment in the Hawaiian region (Dziewonski et al., 1992). At Site 843, Holes 843A and 843B penetrated ~235 m of pelagic and volcanoclastic sediment before reaching oceanic basement. Recovered sediment was classified into three lithologic units defined from the seafloor down: (1) ~20 m of Quaternary to Pliocene silt and clay containing variable amounts of volcanic sand, (2) ~16 m of middle Miocene to upper Eocene clay and claystone with altered volcanic sand, (3) a ‘catch-all’ unit ~200 m thick, composed primarily of chert and claystone (recovery of this unit was poor) (Fig. 2). Volcanic sand within units 1 and 2 were probably emplaced by turbidity currents associated with giant landslides from the Hawaiian ridge (Garcia, 1993). Difficulty imaging the sediment/oceanic basement contact using seismic reflection techniques was attributed to the presence of highly reflective chert layers overlying the oceanic crust (Wilkins et al., 1993).

### 3. Correlation of previous drilling results and seismic reflection data

Re-evaluation of previously collected MCS profiles (Watts et al., 1985; Brocher and ten Brink, 1987) and drilling results from ODP Leg 136 (Dziewonski et al., 1992) allow us to correlate seismic reflection data with lithology on the Southern HA (SHA, Fig. 2). MCS lines collected on R/V *Robert Conrad* Cruise 2308 (RC2308-303 and RC2308-304) cross ODP Sites 842 and 843, located ~250 km southwest of the island of Oahu on an abyssal ridge at ~4400 m water depth (Figs. 1 and 2). Correlation of the seismic data with lithology and physical property logs provides a reference section that can be compared to our data in the Hawaiian Moat. Our re-exami-

nation of the MCS reflection records and drilling results focuses on matching changes in seismic reflection character with lithologic units and variations in physical properties (Fig. 2).

We constrain the location of the oceanic basement by closely examining an in-situ velocity profile from ODP Hole 843A (Fig. 2A). Down-hole logging of Hole 843A determined a P-wave velocity range of 1500–2900 m/s from 50 to 205 m below sea floor (mbsf) in the sediment. Integration of this velocity profile predicts a two-way travel time (twtt) to the basement of  $\sim 260$  ms, assuming velocities of 1650 ( $\pm 50$ ) and 2200 ( $\pm 100$ ) m/s for the shallow and deep portions of the core that were not logged. Similarly, we calculate a twtt of  $\sim 280$  ms to the basement at nearby Hole 843B. Close examination of the seismic reflection record reveals a high-amplitude, roughly continuous, low-frequency (10–25 Hz) reflection occurring at  $\sim 270$  ms twtt that we interpret as originating at the contact between the basement and overlying pelagic sediment (Fig. 2B,C).

Within the sediment that overlies the basement reflection on the SHA, we interpret two seismic units. Immediately below the seafloor reflection, we identify a layer of high-amplitude, stratified, strongly continuous, mid-frequency (20–40 Hz) reflections that thins over basement highs, ponds in basement lows, and varies in thickness from 100 to 150 ms (Fig. 2B,C). We designate these reflections as *seismic* unit HA1 and interpret them to originate from turbidite beds such as those found in ODP *lithologic* units 1 and 2 from Site 842. The velocity profile of ODP Hole 843a establishes the base of unit HA1 at  $\sim 100$  mbsf, within ODP *lithologic* unit 3 (Fig. 2A,C). This suggests that the upper 65 m of ODP unit 3 probably contains turbidite deposits (Fig. 2A). A lithologic boundary at  $\sim 100$  mbsf within ODP unit 3 is consistent with the physical property variations of Hole 843A. Specifically, at 100 mbsf the velocity log shows an increase in the amplitude of high-velocity peaks and the trend of the  $\gamma$  ray log changes from down-hole increasing to down-hole decreasing (Dziewonski et al., 1992) (Fig. 2A). Directly beneath seismic unit HA1 and draping the basement reflection, we identify a region of low-amplitude, weakly contin-

uous, higher frequency (30–45 Hz) reflections that varies in thickness from 150 to 180 ms (Fig. 2B,C). We define these reflections as *seismic* unit HA2 and interpret them to originate from the lower 130 m of ODP *lithologic* unit 3, i.e. pelagic sediments. The identification and correlation of these seismic units with the lithologic data provides important groundtruth for subsequent interpretations of our data.

#### 4. Data acquisition and processing

In January–February 1998, we shot a grid of 29 seismic profiles over the FHM and the submarine flanks of the island of Hawaii on the R/V *Maurice Ewing* towing a 4.2 km, 160 channel streamer cable (Fig. 1). The seismic source was a 71 l (4336 inch<sup>3</sup>) array of 15 airguns fired every 50 m. The data were recorded in SEG-D format, with a sample interval of 2 ms (resampled to 4 ms prior to processing).

Data processing, carried out at the University of Hawaii using ProMAX software, was designed to image both the sediment on the abyssal plain and the internal structure of the volcanic edifice (Table 1). Additional tests performed to enhance reflections and aid interpretation included band-pass filtering, spectral shaping, constant-velocity stacks, and deconvolution (see Hills et al., 2002 for more details).

Table 1  
Standard seismic data processing sequence

Process	Explanation
Edit bad traces	noisy channels removed from data
Geometry	shot/receiver definition
Sort to common mid-point (CMP) gathers	12.5 m CMP spacing - 40-fold
Bandpass filter	4–8–72–80 Hz filter
Velocity analysis	approximately every 100 CMP
Dip move out (DMO)	partial migration algorithm
Top mute	remove noise at far offsets
CMP ensemble stack	
F-K migration	
F-K filter	remove strongly dipping events
Automatic gain control (AGC)	scale amplitude of reflections for display

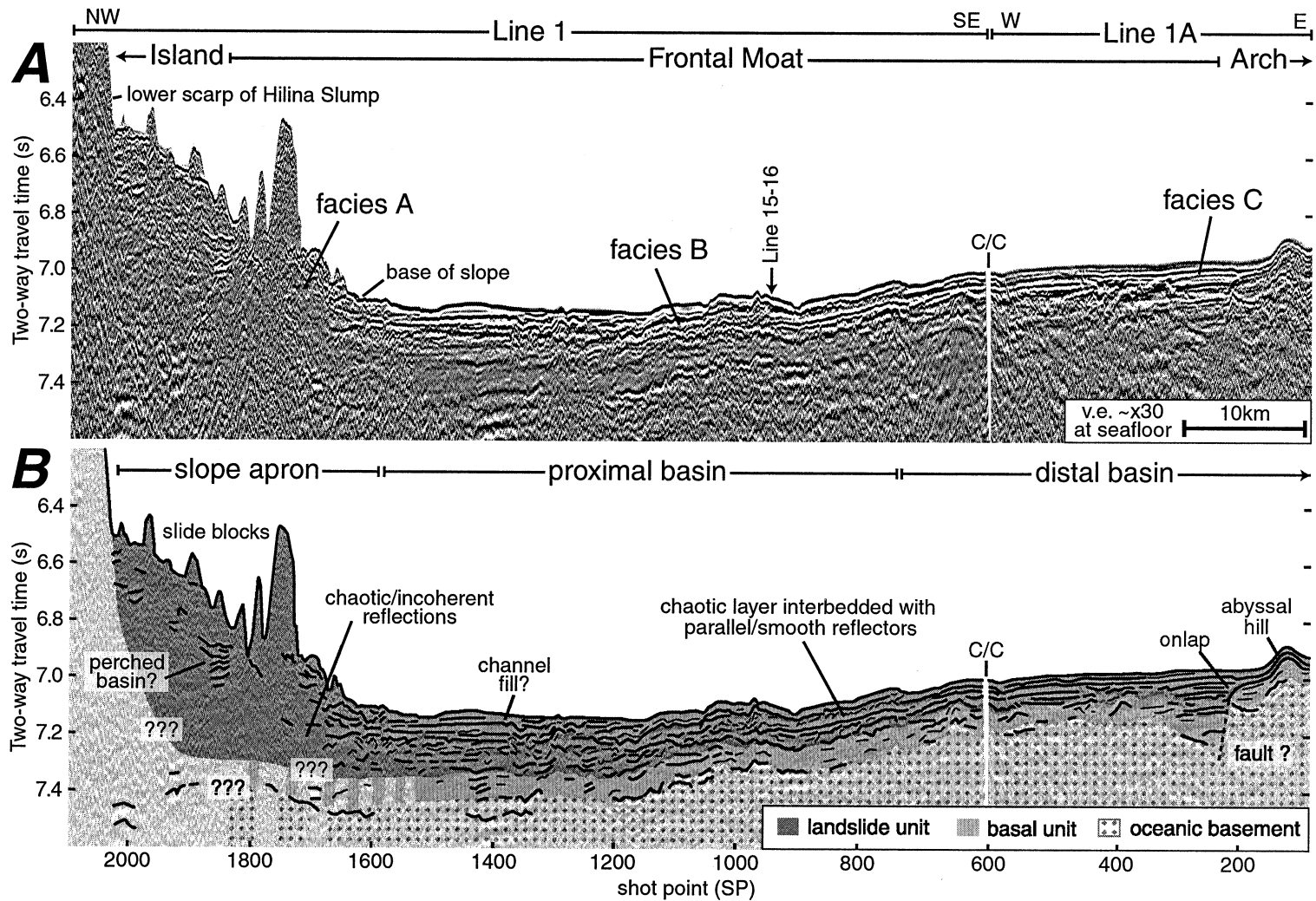


Fig. 3. Seismic reflection line 1 and 1a (A) and interpretation (B). Long (> 100 km) profile crosses the FHM and approaches the FHA. Slope apron contains numerous large slide blocks and only small areas of laterally continuous or coherent reflections. Proximal basin area contains chaotic/hummocky reflectors interpreted as debris flow deposits, bounded by areas of parallel and continuous reflections. Interfingering between chaotic/hummocky reflectors and smoother/parallel sequences of reflections is common in this region. Distal basin is characterized by low basement topography (abyssal hills) and onlapping parallel reflections that infill small basins. Extensive sequences of parallel reflectors are interpreted as turbidite deposits. C/C marks course change of ship from line 1 to line 1a.

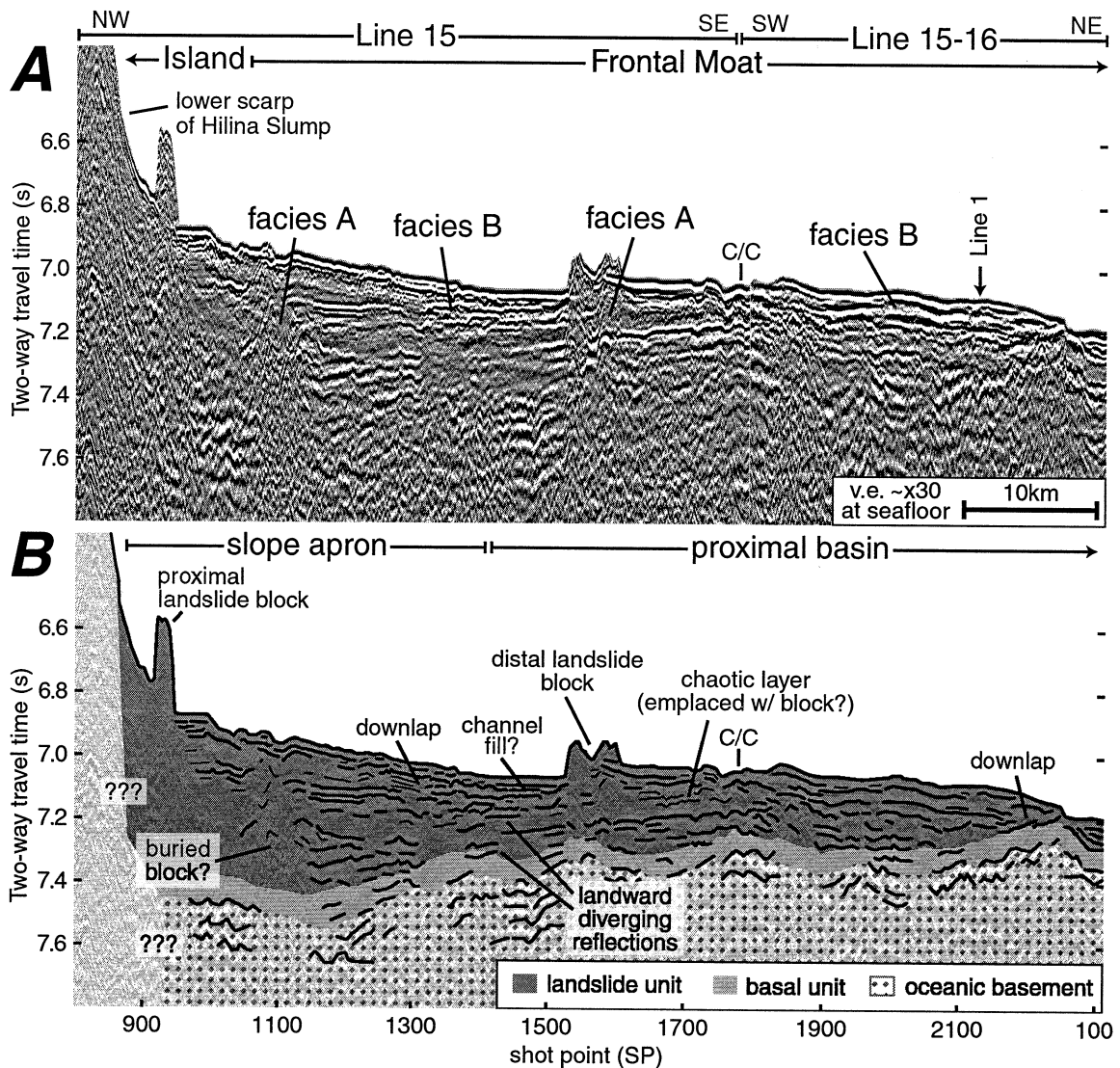


Fig. 4. Seismic reflection line 15 and 15–16 (A) and interpretation (B). Long profile across FHM (compare to Fig. 3). Little expression of the moat exists topographically, but note the landward dipping nature of the top of the oceanic basement. Landward diverging reflectors are possible indicators of continued landward subsidence of the basement. Deeply rooted chaotic region may be a buried block from previous landslide event. Distal blocks with underlying continuous reflectors are present, surrounded by a chaotic layer of reflections. Rapidly thinning landslide unit downlaps underlying horizons in the distal portion of this line. C/C marks course change of ship from line 15 to line 15–16.

## 5. Seismic reflection data: results and interpretation

Within the FHM we recognize a rough and irregular horizon interpreted as the oceanic basement, a basal layer of relatively constant thickness

(~80–100 ms) interpreted as pelagic sediment, and an elongate wedge of onlapping and downlapping reflections interpreted as landslide debris and associated turbidite deposits derived from the nearby Hawaiian Ridge (Figs. 3 and 4). These features are illustrated with two seismic reflection



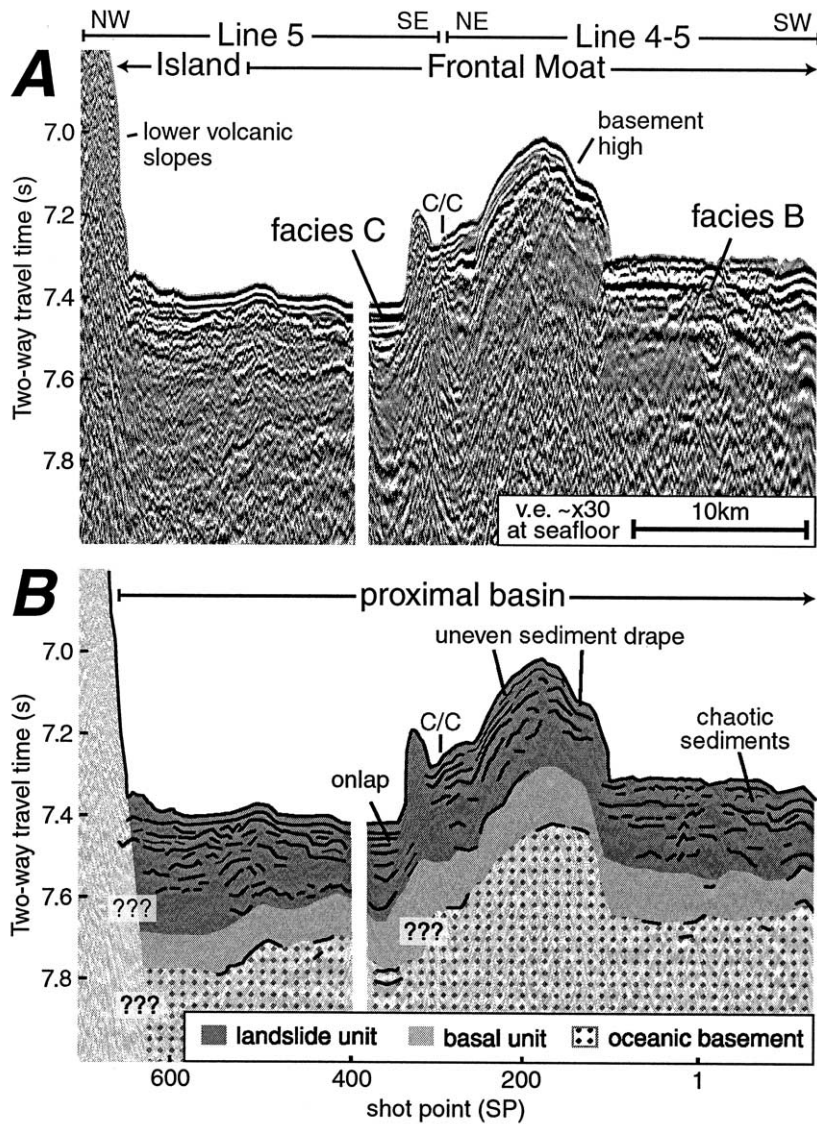


Fig. 5. Seismic reflection line 5 and 4–5 (A) and interpretation (B). Profile images sharp transition from lower volcanic slopes of island to the abyssal sea floor. Note the absence of slope apron adjacent to volcano. Sea floor is dominated by pre-existing basement high. Depth to seafloor is greater on the northern side of the basement high, indicating that the feature may deflect or reflect turbidity currents or debris flows moving along the axis of the FHM. The uneven sediment drape and contrasting facies on either side of basement high are further evidence that sediment deposition is influenced by this feature. C/C marks course change of ship from line 4–5 to line 5.

profiles that extend from the base of the volcanic flank across the axis of the FHM (Figs. 3 and 4). Vertical position on all seismic reflection profiles is referenced to twtt below sea level in seconds (s) and lateral position is denoted by shot point (SP).

### 5.1. Oceanic basement

The top of the Pacific oceanic crust is identified as a poorly continuous reflection that deepens towards the island edifice (Fig. 3, SP 800–1200,

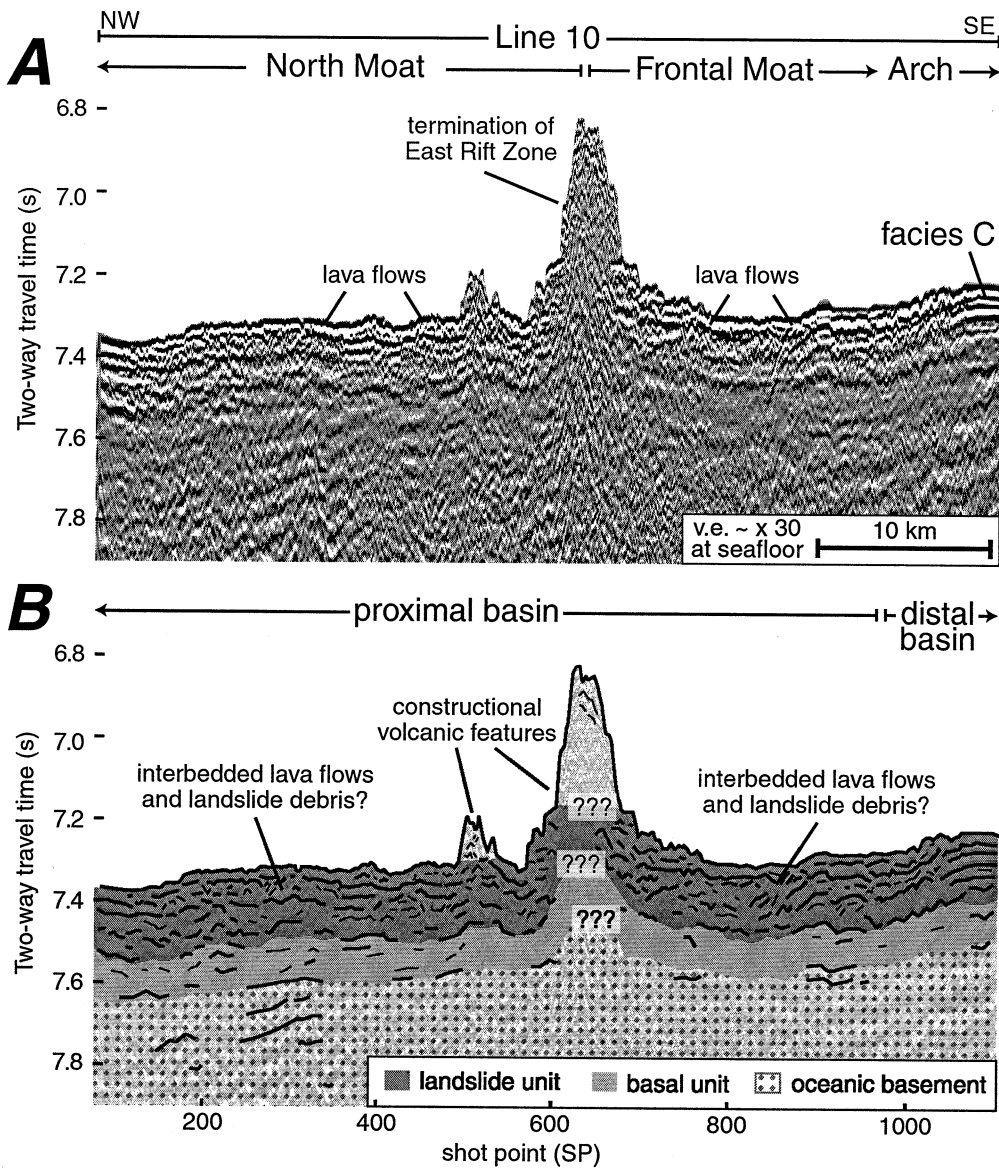


Fig. 6. Seismic reflection line 10 (A) and interpretation (B). Profile crosses the termination of the ERZ of Kilauea, where extensive submarine sheet flows have obscured the sediment record (Holcomb et al., 1988). Interbedding between sediments and lava flows is likely, but the exact nature of this relationship remains poorly resolved. Parallel reflections (facies C) at the SE end of the line signify the transition to the distal basin environment.

~7.4 s and Fig. 4, SP 100–1200, ~7.4 s). This reflection is nearly identical to the basement reflection at ODP Site 843 (Fig. 2). Characteristics which typify the basement reflection include: (1) rough and irregular reflector geometry; (2) under-

lying low-frequency reverberations that mimic basement topography; (3) the region beneath the basement appears free of coherent or continuous reflection events; (4) a distinctive layer of low-amplitude reflections, interpreted as pelagic sedi-

ment (discussed in detail below) that drapes the basement reflection. These basement characteristics are consistent with the observations of previous seismic reflection studies (ten Brink and Watts, 1985; Lindwall, 1988; Rees et al., 1993).

Basement topography throughout the FHM is extremely variable and has a noticeable effect on sediment distribution. Pre-existing seafloor highs present between Hohonu and Green Seamounts are covered by a layer of pelagic sediment and/or turbidite deposits (Fig. 5, SP 50–200, ~7.0–7.3 s). Depth to the abyssal sea floor is ~90 m greater on the northern side of these low relief seamounts than on the southern side, perhaps indicating that they are barriers to sediment transport along the axis of the FHM (Fig. 5, SP 1–400, 7.2–7.4 s). North-northwest trending abyssal hills appear as regions of elevated basement topography with flanking sediment-filled basins (Fig. 3, SP 100, 7.1 s). Large basement highs interpreted by previous workers as Cretaceous age seamounts (e.g. Apuupuu, Hohonu and Green Seamounts) rise hundreds to thousands of meters above the surrounding seafloor (Moore and Chadwick, 1995) (Fig. 1).

### 5.2. Basal unit: pelagic sediment

Draping the oceanic basement is a laterally extensive, weakly reflective layer, 80–100 ms thick, which occurs throughout the FHM. Reflections within the basal unit are low-amplitude, moderately to poorly continuous, and concordant with the upper and lower boundaries of the unit. This unit is well resolved on the inner slope of the Hawaiian Arch (Fig. 3, SP 800–1400, ~7.2–7.4 s) but is difficult to image in other regions of our study area, especially in areas of the Hawaiian Moat covered by submarine lava flows (Fig. 6). We correlate reflection patterns within this unit with the reflections of unit HA2 from seismic reflections surveys on the Hawaiian Arch (Fig. 2). Based upon this correlation, the sheet drape geometry of this unit, the nature of the internal reflections, and previously identified pelagic sediment from the Northern Hawaiian Moat (Rees et al., 1993), we interpret the basal unit as a

layer of pelagic sediment ~80–100 m thick (Winterer, 1989).

### 5.3. Landslide unit: volcanoclastic sediment

Overlying the basement and pelagic sediment layer is a landward-thickening wedge of high-amplitude onlapping reflections (Figs. 3 and 4). The thickness of this wedge is greatest (~700–900 ms) adjacent to large erosional features on the flanks of Loihi seamount and the outer scarp of the Hilina Slump, decreasing rapidly in thickness with distance from these areas. Reflections within the landslide unit are high amplitude and often exhibit landward diverging reflection geometry (Fig. 4B). We interpret this wedge as debris avalanche and debris flow deposits derived from volcanic slope failures. Within the landslide unit, three distinct seismic facies are identified according to changes in seismic reflection character and geometry (Table 2).

#### 5.3.1. Facies A: proximal debris avalanches and slumps

We define facies A as sequences of chaotic/incoherent reflections and irregular blocks found in thick sequences (100–500 ms twtt) adjacent to the steep (> 5°) submarine slopes of Hawaii (Figs. 3 and 4). This facies is common within a wedge or 'slope apron' region flanking the lower slopes of the submarine volcano (discussed below). Although reflections from within this facies are generally chaotic, they locally dip slightly to the SE, away from the volcanic edifice. Large, irregular blocks scattered on the seafloor in this region exhibit few internal reflections and are grouped with this facies. Isolated regions of parallel reflections onlapping these blocks may represent small trapped or 'perched' basins (Fig. 3, SP 1850, 6.9 s).

The distribution of this facies (principally bordering the steep volcanic flanks of Hawaii), the lack of coherent internal reflections, and the frequent occurrence of large blocks indicates that facies A is composed primarily of poorly sorted volcanoclastic debris. The majority of this material was probably derived locally from the lower

slopes of Kilauea and Loihi during slope failure events.

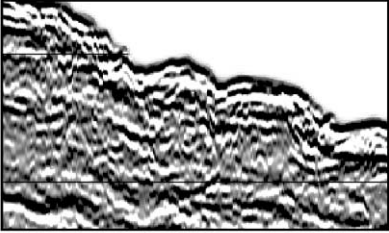
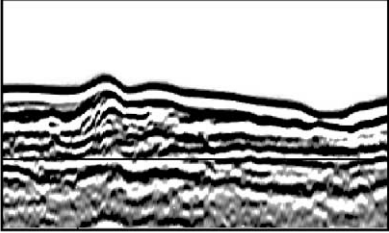
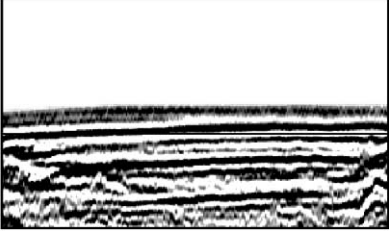
### 5.3.2. Facies B: distal debris avalanches/debris flows

Facies B is characterized by lenses of chaotic and hummocky reflection events that are common within the frontal moat and onlap the frontal arch (Figs. 3 and 4). Thick sequences of these reflections (~400 ms) occur at or near the boundary between the abyssal sea floor and the lowermost slopes of the volcanic edifice (Fig. 4). These reflections become thinner towards the arch and eventually become interbedded with facies C re-

flections (discussed below) (Fig. 3, SP 500–800, 7.0–7.2 s). Individual reflectors within this facies may exhibit a variety of reflection forms. Hummocky subunits are common and may downlap underlying planar horizons. Extremely chaotic and irregular areas are common, often interbedded with smoother, more continuous reflectors (Fig. 3, SP 800, 7.1–7.2 s).

We interpret these hummocky and irregular lenses as the product of chaotic debris avalanches or debris flows originating from the nearby slopes of Hawaii. Chaotic or reflection free areas may represent buried blocks from older catastrophic debris avalanche events, which were subsequently

Table 2  
Seismic reflection facies defined in this study and their geologic interpretation

Seismic facies	Characteristics	Geological Interpretation
 <p>seismic facies A</p>	Highly chaotic/incoherent areas containing few internal reflections, often bordered by continuous reflections	Proximal debris avalanche or lower slump deposits
 <p>seismic facies B</p>	Hummocky and/or chaotic sequences of reflections that thin with distance from the island edifice and onlap or downlap underlying reflections	Distal debris avalanche or debris flow deposits
 <p>seismic facies C</p>	Sequences of continuous, parallel, generally flat-lying reflections that 'pond' in low areas and onlap underlying reflections	Turbidites

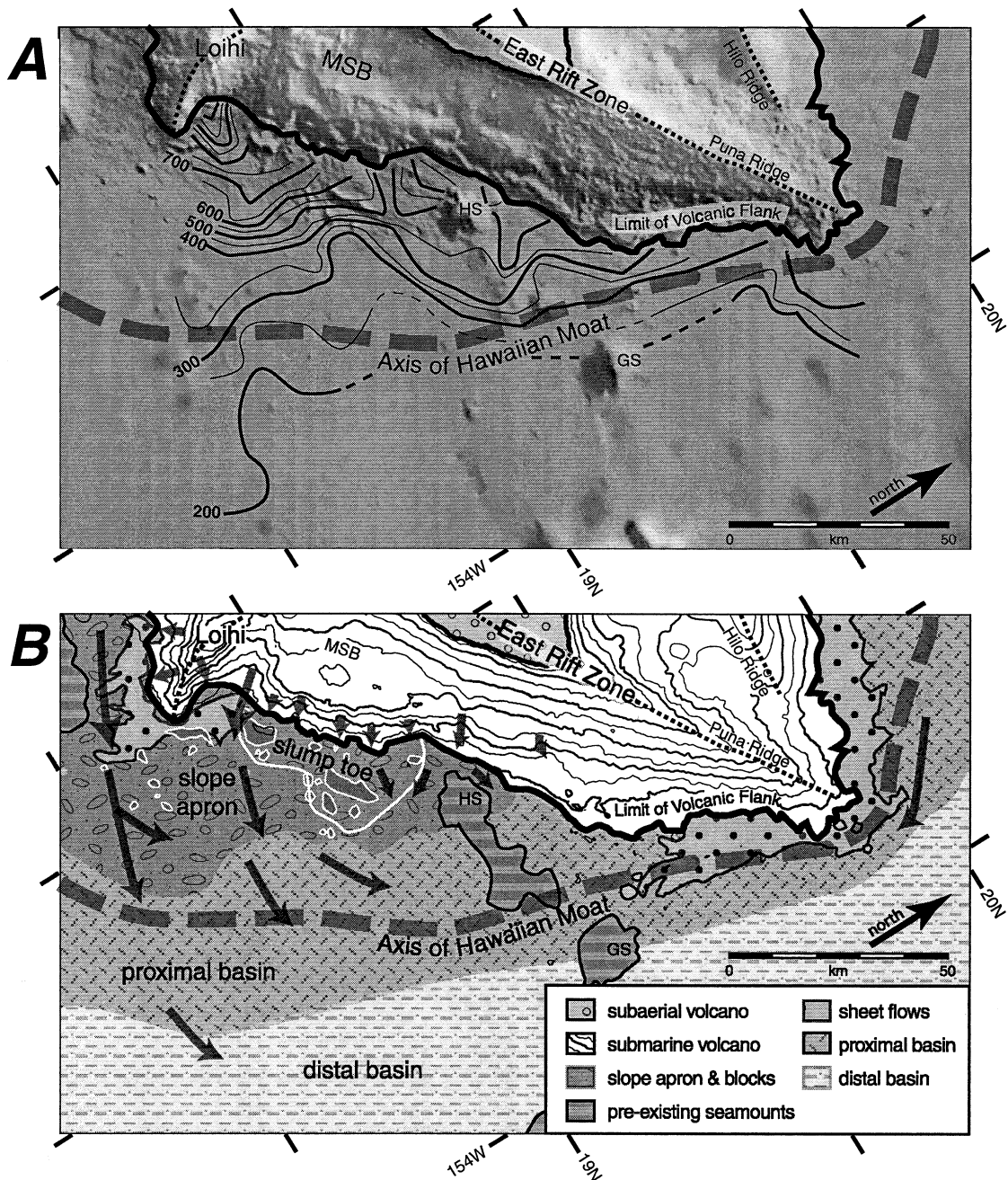


Fig. 7. (A) Shaded relief bathymetric map of FHM with sediment thickness superimposed. Contours in 100 ms of twtt. Dashed contours indicated interpreted thickness. (B) Interpreted sediment pathways (arrows) and depositional regimes. Slump toe region defined by Smith et al. (1999). Stippled pattern indicates submarine sheet flows identified by Holcomb et al. (1988). Submarine topographic features influencing sediment deposition include the mid-slope bench (MSB) of the Hilina Slump, Hohonu Seamount (HS), and Green Seamount (GS). Heavy dark line shows lower limit of volcanic flank. Slope apron, proximal basin, and distal basin are defined by the predominance of facies A, B and C on reflection profiles.

buried by later landslide events (Fig. 4, SP 1100, 7.0–? s).

### 5.3.3. *Facies C: turbidites*

We recognize facies C as a series of generally high-amplitude, high-frequency, continuous reflections that overlie and onlap the top of the basal pelagic sediment unit. In the distal regions of our survey area (e.g. Fig. 3, SP 200–600), this facies is laterally extensive and well-resolved. Thickness varies locally (~60–160 ms) depending upon underlying basement topography. Individual reflections are continuous (some extend laterally for tens of kilometers) and dip gently towards the Hawaiian Ridge. Facies C is overlain by extensive sequences of chaotic reflections (facies A and B) in regions proximal to the volcanic edifice, making it difficult to image in these areas.

We interpret the highly continuous and parallel reflections of facies C as distal turbidite deposits derived from the Hawaiian Ridge during mass-wasting events (cf. Garcia and Hull, 1994). The lateral continuity and onlapping nature of reflections within this unit supports this interpretation. The distribution of this facies appears strongly influenced by basement topography (Fig. 3, SP 200–300) further suggesting current-controlled depositional processes. We note the strong similarity of the internal reflections of this facies and those of unit HA1 (interpreted as turbidites) on the Hawaiian Arch (Fig. 2). In addition, this interpretation is supported by volcanic sands deposited by turbidites collected in two locations (~120 km and ~250 km) to the SE of the island of Hawaii (Naka et al., 2002).

### 5.4. *Sediment distribution*

The volcanoclastic sediment identified in our study is distributed unevenly throughout the frontal moat, with a thick accumulation of sediment occurring adjacent to the outer scarp of the Hilina Slump that thins with increasing distance from the volcanic slopes (Fig. 7A). For the purposes of description, we divide the FHM into three distinct regions: (1) slope apron; (2) proximal basin; and (3) distal basin (Fig. 7B). The slope apron forms a wedge of material abutting the lower slopes of

Loihi and the Hilina Slump (Fig. 4). The top boundary of the slope apron is the seafloor, which dips slightly (<2.5°) away from the island towards the axis of the deep and is characterized by a blocky-hummocky surficial morphology. The slope apron reaches a maximum thickness of ~800 ms (~1.2–1.4 km) at its landward boundary, thins rapidly towards the axis of the Hawaiian moat, and pinches out at the abyssal plain sea floor (Fig. 7). The surficial area of the slope apron encompasses the previously described ‘lower toe’ of the Hilina Slump (Smith et al., 1999). The proximal basin is a transition area between the blocky-chaotic area of the slope apron and the smooth-parallel reflections of the distal basin. This region is typified by relatively continuous hummocky reflection units, interbedded with smooth and parallel reflections (Fig. 3). The distal basin area is dominated by turbidite deposition and is characterized by a thin accumulation of onlapping, parallel reflections (Fig. 3).

## 6. Discussion

### 6.1. *Depositional processes and sediment pathways*

Our results indicate that deposits from mass-wasting processes have contributed >1200 km<sup>3</sup> of sediment to our survey area within the FHM, forming a prograding volcanoclastic depositional system (Fig. 7). The variable distribution of these deposits reflects proximity of the sediment source, changes in mode of deposition, and the effects of seafloor topography. The thick accumulation of landslide debris at the slope apron demonstrates that a significant portion of material shed from the volcanic slopes remains relatively close (<30 km) to the source region. Slumps, debris avalanches, and turbidites represent processes along a continuum of landslide events that transport sediment from the volcanic slopes of the island into the Hawaiian Moat. Original seafloor topography (i.e. abyssal hills and seamounts), along with recently emplaced landslide blocks, appears to deflect or reflect bottom currents responsible for sediment transport and deposition (Fig. 5).

Fig. 7B schematically illustrates the main fea-

tures observed in the frontal moat and pathways of sediment transport. The likely source of the majority of the slope apron material is the slopes of Kilauea, Mauna Loa, and Loihi volcanoes. Amphitheater valleys on the slopes of Loihi (Fornari et al., 1988) and slide scars on the outer Hilina scarp of Kilauea (Smith et al., 1999) provide evidence for mass-wasting events that emplaced large detached blocks lying on the abyssal seafloor. Present day sediment transport pathways are inferred from erosional features, bathymetry, and sediment accumulation within the FHM.

Older volcanoes such as Haleakala, Kohala, Mauna Loa and Mauna Kea have also contributed sediments to this area during earlier slope failure events (Lipman et al., 2000; Naka et al., 2002). Kanamatsu et al. (2002) dated turbidite layers in a piston core located ~250 km southeast of the island of Hawaii at 0.78 Ma or older. These ages predate any published volcano ages for the island of Hawaii (Clague and Dalrymple, 1987), suggesting sources from volcanoes on older islands.

The distribution of slump, debris avalanche, and turbidite deposits demonstrates the interrelationship among mass-wasting processes during the transport of material from the volcanic slopes to the FHM. The emplacement of large blocks during debris avalanche events was likely accompanied by reworking and entrainment of seafloor sediments, high energy distal debris flows, and turbidity currents. Distal debris flow and turbidite deposits dominate a broad, poorly defined region seaward of the base of the volcano centered around the axis of the FHM. These distal debris avalanche and turbidite deposits were probably emplaced contemporaneously with the larger blocks of the slope apron and chaotic debris avalanche deposits of the proximal basin. The lateral gradation of distal debris avalanche deposits into predominantly turbidite deposits is consistent with this relationship (Fig. 3, SP 400–800, 6.9–7.2 s). Turbidite deposits may occur throughout the survey area and at distances >80 km from the sediment source region appear to be the primary type of landslide-derived sediment. These distal turbidite deposits are probably the product of catastrophic slope failures of older Hawaiian

volcanoes that have since passed the shield-building stage (Garcia and Hull, 1994; Kanamatsu et al., 2002). They were likely emplaced at the same time as thicker debris avalanche deposits now buried beneath the island of Hawaii.

Turbidity current deposits are influenced by regional variations in topography (Pickering et al., 1992; Kneller and McCaffrey, 1999; Bursik and Woods, 2000). Density flows may be reflected or deflected by topographic features and decoupling of denser and less dense portions of the flow may occur (Kneller and McCaffrey, 1999), although turbidity currents can climb significant topographic slopes (Muck and Underwood, 1990). In the FHM, seafloor topography noticeably affects sediment distribution, particularly the distribution of turbidite and distal debris avalanche deposits. Turbidity currents and debris avalanches travel downslope away from the volcanic edifice until they reach the abyssal sea floor. It is likely that sediment flow patterns become highly complex within the proximal basin, as has been shown in other linear, deep-marine basin environments (Pickering et al., 1992). Sequences of nearly horizontal reflectors (along moat channel deposits?) are visible at the axis of the deep on several lines (Figs. 3 and 4). They typically onlap underlying chaotic reflections and may result from depositional currents that travel along the axis of the moat. These thin horizontal reflections are the youngest sediments deposited in the moat and are analogous to unit 4 of Rees et al. (1993). A facies change across a topographic feature (interpreted as a small Cretaceous seamount) may indicate a decoupling of basal portions of debris flows from less dense, finer grained parts of the flows as they travel to the north along the axis of the FHM (Fig. 5). The differential in seafloor depth across this barrier (deepening to the north) is evidence of this sediment damming. Larger relief features, such as Hohonu Seamount or previously emplaced avalanche blocks, provide much larger barriers to sediment transport, with large volumes of sediment being rerouted or reflected by these features (Fig. 7). Sediment influx into the FHM from the slopes of Kilauea may have decreased since the growth of the mid-slope bench, which forms a closed basin that traps hy-

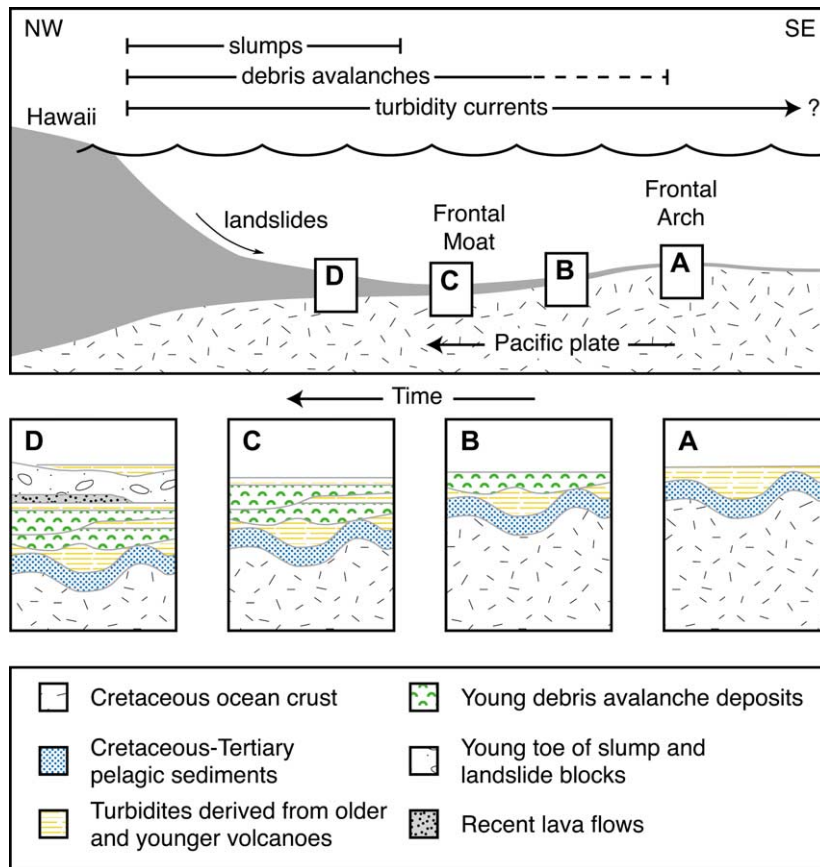


Fig. 8. Schematic depiction of the predicted stratigraphy of the Hawaiian Moat and Arch to the southeast of the island of Hawaii (top portion of figure modified from Garcia and Hull, 1994). Locations of profiles A–D are shown as insets. (A) Turbidites and pelagic sediments on the Hawaiian Arch. (B) Gradually thicker volcanoclastic deposits approaching the FHM. (C) Debris avalanche and turbidity current deposits dominate along the axis of the FHM. (D) Thickest accumulation of sediments overlain by slump deposits predicted at the toe of the volcanic edifice.

aloclastic sediment shed from the subaerial part of the island.

## 6.2. Stratigraphic model

The spatial distribution of sediment within the FHM reflects the relationship between depositional processes, volcanic evolution, and the tectonic forces of plate motion and lithospheric flexure. Continual degradation of the leading edge of the Hawaiian Ridge feeds clastic material into the FHM that is subsequently buried beneath new volcanic centers. The northwest motion of the Pacific Plate moves previously distal regions of the plate closer to the location of new volcanic cen-

ters, where the rate of volcanoclastic sediment input is high. Continued lithospheric flexure, coupled with plate motion, results in the migration of the FHM to the southeast along with the prograding volcanic chain. Thus, older, now dormant or extinct Hawaiian volcanoes likely contributed sediments to the present day FHM.

The interaction of tectonic forces and depositional processes should result in a predominantly *coarsening-upward* stratigraphy within the frontal moat (Fig. 8). We hypothesize a lithostratigraphic sequence grading upward from pelagic sediment, into turbidite deposits, followed by distal debris flow deposits, and finally proximal debris avalanche deposits. Lava flows may be interbedded



within the upper portion of this sequence, especially near the terminal regions of volcanic rift zones. The existence of a thick accumulation of sediment adjacent to Loihi, which represents a very early stage of Hawaiian volcanism, implies that sediment deposits exist on the abyssal seafloor preceding the growth of new volcanoes, forming a basal layer of volcanoclastic material underneath the Hawaiian Ridge (e.g. Moore and Clague, 1992). Ultimately, seaward sliding of the submarine flanks by volcanic spreading may override or incorporate the depositional sequence at the flank toe. Local variations in the magnitude or location of the mass failure events result in the overlapping and interfingering of debris avalanche and turbidite sequences (e.g. Fig. 3, SP 400–800, ~6.9–7.2 s).

### 6.3. Regional and global comparisons

Basic differences between the FHM and the flanking segments of the Hawaiian Moat include relative age, topographic relief, and depositional history. As stated previously, the FHM is a relatively short-lived feature that migrates with successive volcanic loads. In contrast, the flanking segments of the Hawaiian Moat are essentially permanent features that fill with sediment over time. Moat to arch relief within the flanking moat segments can be >1 km while in the FHM it is ~200–450 m, indicating less subsidence of the ocean crust in the frontal region. In addition, sediment in the flanking moats is much thicker, implying a greater influx of sediment and longer depositional history. In the Northern Hawaiian Moat, landslide debris has been grouped into landslide, offlapping and ponded units (units 2, 3 and 4 of Rees et al., 1993) based upon reflection geometry and stratigraphic relationships. The formation of these distinctive units is ascribed to the competing effects of sediment influx and flexural subsidence due to the progressive growth and degradation of new volcanic centers (Rees et al., 1993). The landslide unit we describe within the FHM exhibits characteristics of all three units identified from the Northern Hawaiian Moat, but we are unable to further subdivide it.

The FHM and associated sediments clearly represent an early stage of moat evolution. The sedimentary history of the flanking moat was divided into four stages by Rees et al. (1993): (1) initial moat formation; (2) lower landslide unit formation; (3) deposition of main landslide unit and offlapping unit; and (4) formation of a ponded unit. They state that in the initial stage of formation (stage 1) that older mass-wasting events or their ‘fringing turbidites’ are not yet depositing sediments within the flexural moat. In contrast, we interpret turbidite deposits within the distal basin of the FHM and note that turbidite layers in piston cores have been recovered up to 250 km SE of the island of Hawaii (Naka et al., 2002). Within the area we define as the proximal basin, the landslide unit we image corresponds to stage 2, the ‘lower landslide unit formation’ of Rees et al. (1993). However, the sediments we image within the FHM will likely be buried by a new volcano rather than form the lower portion of a thick sedimentary sequence.

The stratigraphic model we propose for the leading edge of the Hawaiian Ridge is also applicable to other oceanic hotspot traces. The giant landslide deposits of the Hawaiian Ridge are often compared to those of other oceanic volcanic chains such as the Marquesas or the Canary Islands (Filmer et al., 1994; Gee et al., 2001). Similarities between these three island chains include: (1) a general linear age progression of the islands; and (2) thick accumulations of landslide debris surrounding the islands. Unlike the Hawaiian Islands, the Marquesas Islands are surrounded by an ‘archipelagic apron’ (Menard, 1956) resulting from extensive mass wasting of the islands overflowing the flexural moat that surrounds the islands (Filmer et al., 1993; Wolfe et al., 1994). In contrast, the youngest islands of the Canaries (Las Palmas and El Hierro) exhibit no apron or flexural moat, perhaps because they are too small or too recent to have generated much sediment, or to have had a significant loading effect on the underlying crust (Gee et al., 2001). Despite the differences between these island chains, sediment deposited in the path of these ‘prograding’ volcanoes should exhibit a coarsening-upward stratigraphy, reflecting the migration of the volcanic

load across the underlying plate and widespread mass wasting of the submarine volcanic flanks.

#### 6.4. Tectonic implications

One objective of this study was to assess the distribution of moat sediments in order to evaluate conceptual models of volcanic flank failure along a nearly horizontal detachment. Flank mobility has been examined by previous studies using limit-equilibrium analyses of wedge-shaped slices of volcanic flanks to test the likelihood of flank failure (Dieterich, 1988; Iverson, 1995). Iverson (1995) treated buried sediment beneath the volcanic edifice as a uniform layer of pelagic clay of low hydraulic diffusivity. Assuming a thin (20 m) layer of pelagic clay in his modeling, he concluded that flank failure was not possible under static loading conditions and that a much thicker (200 m) layer would be necessary to allow slip. Our results indicate that the actual thickness of the pelagic layer (assuming a 'typical' sediment velocity of 2000 m/s) is 80–100 m thick, approaching the 200-m thickness hypothesized by Iverson. Moreover, if the thick accumulations of volcaniclastic debris we recognize within the Frontal Moat also extend beneath the volcano, they could define a layer of low strength material, hundreds of meters thick, upon which the flanks of the volcano may slide. This sediment layer is most likely highly variable in thickness and composition, possibly containing large landslide blocks from previous mass failures. Locally, basement topography such as seamounts may pierce through the sediment layer, providing resistance to flank sliding (e.g. Smith et al., 1999). The presence of such a thick sediment layer beneath the volcanic edifice agrees with a low-velocity layer inferred beneath the flanks of Mauna Loa (Thurber and Li, 1989). The proposed thickness of this low-velocity layer (800 m) is consistent with our observations for the thickness of slope apron deposits within the FHM.

#### 7. Conclusions

Seismic reflection data image sediments lying

on the sea floor to the southeast of the island of Hawaii. Based upon their seismic reflection character, we identify two primary sedimentary units: (1) a basal layer of primarily pelagic sediment draping the Cretaceous age igneous basement and (2) a wedge of volcaniclastic material infilling the FHM and overlapping the FHA. Within the volcaniclastic unit we identify three seismic facies that we interpret as (A) proximal debris avalanche and lower slump deposits abutting the base of the volcanic edifice; (B) a chaotic accumulation of hummocky debris avalanche deposits interbedded with turbidite deposits and (C) a distal accumulation of volcaniclastic turbidite deposit.

The distribution of these sediments is largely a function of proximity to sediment sources, the mode of deposition, and the effects of local topography. The primary modern source for these sediments is the oversteepened lower slopes of Kilauea's Hilina Slump and Loihi volcano. Older volcanoes have undoubtedly contributed to the sediment layer. Plate motion plays an important function in the stratigraphy of the FHM, as distal regions are brought closer to the locus of the Hawaiian hot spot. The interplay of depositional processes and tectonic forces should result in a distinctive coarsening-upward stratigraphic sequence. This characteristic sequence is globally applicable to other hot-spot related volcanic island chains. The combined thickness of sedimentary layers, after burial beneath the volcanic edifice, may provide a notably thick layer of low strength material upon which volcanic spreading may occur.

#### Acknowledgements

This study was supported by the National Science Foundation grant OCE-9711715. We thank the shipboard scientific party and professional crew of the R/V *Maurice Ewing*. R/V *Robert Conrad* seismic lines were kindly provided by Joyce Alsop at LDEO. This research used data provided by the ODP. We acknowledge the support of this research by Landmark Graphics Corporation via the Landmark University Grant Program. Reviews given by J. Caplan-Auerbach,

M. Garcia, D. Masson, M. Underwood, R. Urgeles and C. Wolfe contributed significantly to the improvement of this manuscript. SOEST contribution 5846.

## References

- Borgia, A., 1994. Dynamic basis of volcanic spreading. *J. Geophys. Res.* 99, 17791–17804.
- Brocher, T.M., ten Brink, U.S., 1987. Variations in oceanic layer 2 elastic velocities near Hawaii and their correlation to lithospheric flexure. *J. Geophys. Res.* 92, 2647–2661.
- Bursik, M.I., Woods, A.W., 2000. The effects of topography on sedimentation from particle-laden turbulent density currents. *J. Sediment. Res.* 70, 53–63.
- Clague, D.A., Dalrymple, G.B., 1987. The Hawaiian-Emperor Volcanic Chain, Part I. In: Decker, R.W., Wright, T.L., Stauffer, P.H. (Eds.), *Volcanism in Hawaii*, vol. 1. US Geol. Surv. Prof. Paper 1350, pp. 5–73.
- Dalrymple, G., Silver, E., Jackson, A., 1973. Origin of the Hawaiian Islands. *Am. Sci.* 61, 294–308.
- Denlinger, R.P., Okubo, P., 1995. Structure of the mobile south flank of Kilauea Volcano, Hawaii. *J. Geophys. Res.* 100, 24499–24507.
- de Voogd, B., Palome, S.P., Hirn, A., Charvis, P., Gallart, J., Rousset, D., Danobeitia, J., Perroud, H., 1999. Vertical movements and material transport during hotspot activity: seismic reflection profiling offshore La Reunion. *J. Geophys. Res.* 104, 2855–2874.
- Dieterich, J.H., 1988. Growth and persistence of Hawaiian volcanic rift zones. *J. Geophys. Res.* 93, 4258–4270.
- Dziewonski, A.M., Wilkens, R.H., Firth, 1992. Proc. ODP, Init. Reports, Vol. 136. Ocean Drilling Program, College Station, TX.
- Ewing, J., Ewing, M., Aitken, T., Ludwig, W.J., 1968. North Pacific Sediment Layers Measured by Seismic Profiling. In: Knopoff, L., Drake, C.L., Hart, P.J. (Eds.), *The Crust and Upper Mantle of the Pacific Area*. *Geophys. Mon. Ser.*, vol. 12, pp. 147–173.
- Filmer, P.E., McNutt, M.K., Webb, H.F., Dixon, D.J., 1994. Volcanism and archipelagic aprons in the Marquesas and Hawaiian Islands. *Mar. Geophys. Res.* 16, 385–406.
- Filmer, P.E., McNutt, M.K., Wolfe, C.J., 1993. Elastic thickness of the lithosphere in the Marquesas and the Society Islands. *J. Geophys. Res.* 98, 19565–19577.
- Fornari, D.J., Garcia, M.O., Tyce, R.C., Gallo, D.G., 1988. Morphology and structure of Loihi Seamount based on Seabeam sonar mapping. *J. Geophys. Res.* 93, 15227–15238.
- Funck, T., Lykke-Anderson, H., 1998. Seismic structure of the volcanic apron North of Gran Canaria. In: Weaver, P.P.E., Schmincke, H.-U., Firth, J.V., Duffield, W. (Eds.), *Proc. ODP Sci. Results*, vol. 157. Ocean Drilling Program, College Station, TX, pp. 11–27.
- Funck, T., Schmincke, H.-U., 1998. Growth and destruction of Gran Canaria deduced from seismic reflection and bathymetric data. *J. Geophys. Res.* 103, 15393–15407.
- Garcia, M.O., 1993. Pliocene–Pleistocene volcanic sands from Site 842: products of giant landslides. In: Wilkens, R., Firth, J., Bender, J. (Eds.), *Proc. ODP Sci. Results*, vol. 136. Ocean Drilling Program, College Station, TX, pp. 53–63.
- Garcia, M.O., Hull, D.M., 1994. Turbidites from giant Hawaiian landslides: results from Ocean Drilling Program Site 842. *Geology* 22, 159–162.
- Gee, M.J.R., Watts, A.B., Masson, D.G., Mitchell, N.C., 2001. Landslides and the evolution of El Hierro in the Canary Islands. *Mar. Geol.* 177, 271–293.
- Hamilton, E.L., 1957. Marine geology of the southern Hawaiian Ridge. *Geol. Soc. Am. Bull.* 68, 1011–1026.
- Hills, D.J., Morgan, J.K., Moore, G.F., Leslie, S.C., 2002. Structural variability along the submarine south flank of Kilauea volcano, Hawaii, from a multichannel seismic reflection survey. In: Takahashi, E., Lipman, P.W., Garcia, M.O., Naka, J., Aramaki, S. (Eds.), *Hawaiian Volcanoes: Deep Underwater Perspectives*. AGU Monograph, 128, 51–64.
- Holcomb, R.T., Moore, J.G., Lipman, P.W., Belderson, R.H., 1988. Voluminous submarine lava flows from Hawaiian volcanoes. *Geology* 16, 400–404.
- Iverson, R.M., 1995. Can magma-injection and groundwater forces cause massive landslides on Hawaiian volcanoes? In: Ida, Y., Voight, B. (Eds.), *Models of Magmatic Processes and Volcanic Eruptions*. *J. Volcanol. Geotherm. Res.* 66, 295–308.
- Kanamatsu, T., Herrero-Bervera, E., McMurtry, G.M., 2002. Magnetostratigraphy of deep-sea sediments from piston cores adjacent to the Hawaiian Islands: implications for ages of turbidites derived from submarine landslides. In: *Evolution of Hawaiian Volcanoes: Recent Progress in Deep Underwater Research*. AGU Monograph, in press.
- Kneller, B., McCaffrey, W., 1999. Depositional effects of flow nonuniformity and stratification within turbidity currents approaching a bounding slope: deflection, reflection, and facies variation. *J. Sediment. Res.* 69, 980–991.
- Lindwall, D.A., 1988. A two-dimensional seismic investigation of crustal structure under the Hawaiian Islands near Oahu and Kauai. *J. Geophys. Res.* 93, 12107–12122.
- Lipman, P.W., Sisson, T.W., Ui, T., Naka, J., 2000. In search of ancestral Kilauea volcano. *Geology* 28, 1079–1082.
- Lucci, R.G., Kidd, R.B., 1998. Sediment provenance and turbidity current processes at the Lamenti Seamounts and Stromboli Canyon, SE Tyrrhenian Sea. *Geo-Mar. Lett.* 18, 155–164.
- Macdonald, K.C., Fox, P.J., Alexander, R.T., Pockalny, R., Gente, P., 1996. Volcanic growth faults and the origin of Pacific abyssal hills. *Nature* 380, 125–129.
- Masson, D.G., Canals, M., Alonso, B., Urgeles, R., Huhnerbach, V., 1998. The Canary Debris Flow: source area morphology and failure mechanisms. *Sedimentology* 45, 411–432.

- Menard, H.W., 1956. Archipelagic aprons. *Bull. Am. Assoc. Petrol. Geol.* 40, 2195–2210.
- Menard, H.W., 1964. *Marine Geology of the Pacific*. McGraw-Hill, New York.
- Moore, J.G., Chadwick, W.W., Jr., 1995. Offshore geology of Mauna Loa and adjacent areas, Hawaii. In: Rhodes, J.M., Lockwood, J.P. (Eds.), *Mauna Loa revealed: Structure, Composition, History, and Hazards*. *Geophys. Monograph* 92, pp. 21–44.
- Moore, J.G., Clague, D.A., 1992. Volcano growth and evolution of the island of Hawaii. *Geol. Soc. Am. Bull.* 104, 1471–1484.
- Moore, J.G., Clague, D.A., Holcomb, R.T., Lipman, P.W., Normark, W.R., Torresan, M.E., 1989. Prodigious submarine landslides on the Hawaiian Ridge. *J. Geophys. Res.* 94, 17465–17484.
- Moore, J.G., Normark, W.R., Holcomb, R.T., 1994. Giant Hawaiian landslides. *Annu. Rev. Earth Planet. Sci.* 22, 119–144.
- Morgan, J.K., Moore, G.F., Hills, D.J., Leslie, S.C., 2000. Overthrusting and sediment accretion along Kilauea's mobile south flank, Hawaii: evidence for volcanic spreading from marine seismic reflection data. *Geology* 28, 667–670.
- Morgan, W.J., 1971. Convection plumes in the lower mantle. *Nature* 230, 42–42.
- Muck, M.T., Underwood, M.B., 1990. Upslope flow of turbidity currents: a comparison among field observations, theory, and laboratory models. *Geology* 18, 54–57.
- Naka, J., Kanamatsu, T., Lipman, P.W., Sisson, T.W., Tsuboyama, N., Morgan, J.K., Smith, J.R., Ui, T., 2002. Deep-sea volcanoclastic sedimentation around the southern flank of Hawaii Island. In: Takahashi, E., Lipman, P.W., Garcia, M.O., Naka, J., Aramaki, S. (Eds.), *Hawaiian Volcanoes: Deep Underwater Perspectives*. *AGU Monograph*, 128, 29–50.
- Nakamura, K., 1980. Why do long rift zones develop in Hawaiian volcanoes; a possible role of thick oceanic sediments. *Bull. Volcanol. Soc. Jpn.* 25, 255–269.
- Ollier, G., Cochonat, P., Lénat, J.F., Labzuy, P., 1998. Deep-sea volcanoclastic sedimentary systems: an example from La Fournaise volcano, Réunion Island, Indian Ocean. *Sedimentology* 45, 293–330.
- Pickering, K.T., Underwood, M.B., Taira, A., 1992. Open-ocean to trench turbidity-current flow in the Nankai Trough: flow collapse and reflection. *Geology* 20, 1099–1102.
- Rees, B.A., Detrick, R.S., Coakley, B.J., 1993. Seismic stratigraphy of the Hawaiian flexural moat. *Geol. Soc. Am. Bull.* 105, 189–205.
- Rehm, E., Halbach, P., 1982. Hawaiian-derived volcanic ash layers in equatorial northeastern Pacific sediments. *Mar. Geol.* 50, 25–40.
- Smith, J.R., Malahoff, A., Shor, A.N., 1999. Submarine geology of the Hilina Slump and morpho-structural evolution of Kilauea Volcano, Hawaii. *J. Volcanol. Geotherm. Res.* 94, 59–88.
- ten Brink, U.S., Watts, A.B., 1985. Seismic stratigraphy of the flexural moat flanking the Hawaiian Islands. *Nature* 317, 421–424.
- Thurber, C.H., Li, Y., 1989. Seismic detection of a low-velocity layer beneath the southeast flank of Mauna Loa, Hawaii. *Geophys. Res. Lett.* 16, 649–652.
- Urgeles, R., Canals, M., Baraza, J., Alonso, B., 1998. Seismostratigraphy of the western flanks of El Hierro and La Palma (Canary Islands): a record of Canary Islands volcanism. *Mar. Geol.* 146, 225–241.
- Varnes, D.J., 1978. Slope movement types and processes. In: Schuster, R.L., Krizek, R.J. (Eds.), *Landslides, Analysis and Control*, Special Report 176. National Academy of Sciences, Washington, DC, pp. 11–33.
- Waggoner, D.G., 1993. The age and alteration of Central Pacific Oceanic Crust near Hawaii, Site 843. In: Wilkens, R., Firth, J., Bender, J. (Eds.) *Proc. ODP Sci. Results*, vol. 136. Ocean Drilling Program, College Station, TX, pp. 119–132.
- Watts, A.B., Masson, D.G., 1995. A giant landslide on the north flank of Tenerife, Canary Islands. *J. Geophys. Res.* 100, 24487–24498.
- Watts, A.B., ten Brink, U.S., Buhl, P., Brocher, T.M., 1985. A multichannel seismic study of lithospheric flexure across the Hawaiian-Emperor seamount chain. *Nature* 315, 105–111.
- Wilkens, R.H., Christensen, N.I., Collins, J.A., 1993. Seismic properties and reflectivity of North Pacific ocean cherts. In: Wilkens, R., Firth, J., Bender, J. (Eds.), *Proc. ODP Sci. Results*, vol. 136. Ocean Drilling Program, College Station, TX, pp. 99–104.
- Winterer, E.L., 1989. Sediment thickness map of the Northeast Pacific. In: Winterer, E.L., Hussong, D.M., Decker, R.W. (Eds.), *The Geology of North America*, vol. N, The Eastern Pacific Ocean and Hawaii. *Decade of North American Geology*, *Geol. Soc. Am.*, pp. 307–310.
- Wolfe, C.J., McNutt, M.K., Detrick, R.S., 1994. The Marquesas archipelagic apron: Seismic stratigraphy and implications for volcano growth, mass wasting, and crustal underplating. *J. Geophys. Res.* 99, 13591–13608.